

Coupling between air travel and climate

Kristopher B. Karnauskas^{1*}, Jeffrey P. Donnelly¹, Hannah C. Barkley² and Jonathan E. Martin³

The airline industry closely monitors the midlatitude jet stream for short-term planning of flight paths and arrival times. In addition to passenger safety and on-time metrics, this is due to the acute sensitivity of airline profits to fuel cost. US carriers spent US\$47 billion on jet fuel in 2011, compared with a total industry operating revenue of US\$192 billion. Beyond the timescale of synoptic weather, the El Niño/Southern Oscillation (ENSO), Arctic Oscillation (AO) and other modes of variability modulate the strength and position of the Aleutian low and Pacific high on interannual timescales, which influence the tendency of the exit region of the midlatitude Pacific jet stream to extend, retract and meander poleward and equatorward^{1–3}. The impact of global aviation on climate change has been studied for decades owing to the radiative forcing of emitted greenhouse gases, contrails and other effects^{4,5}. The impact of climate variability on air travel, however, has only recently come into focus, primarily in terms of turbulence^{6,7}. Shifting attention to flight durations, here we show that 88% of the interannual variance in domestic flight times between Hawaii and the continental US is explained by a linear combination of ENSO and the AO. Further, we extend our analysis to CMIP5 model projections to explore potential feedbacks between anthropogenic climate change and air travel.

The northeastern subtropical Pacific between Hawaii and the continental US is a major corridor of long-distance commercial air travel. The AirTime statistic (wheels-up to wheels-down) for roughly 250,000 flights between Honolulu (HNL) and Los Angeles (LAX), San Francisco (SFO), and Seattle–Tacoma (SEA) from 1995 to 2013 by four major carriers (United Airlines (UA), American Airlines (AA), Delta Airlines (DL), and Hawaiian Airlines (HA)) are analysed and compared with observed⁸ daily zonal winds at roughly cruising altitude (300 mb; Fig. 1a). To isolate the signal associated with atmospheric variability (as opposed to systematic changes in traffic, technology or policy), rather than analysing flight times in one direction or the other, the difference between westbound and eastbound flight times (ΔT) of each route is computed. There is substantial seasonal-to-interannual variability (~ 1 h) in monthly smoothed records of ΔT , which is remarkably consistent across different routes and carriers (Fig. 1b). For example, the ΔT records for the HNL–LAX route exhibit correlations of 0.91 (DL versus HA) to 0.95 (UA versus DL). ΔT records for a given route are also significantly correlated with other routes for the same carrier; the HNL–LAX route is correlated 0.86 with HNL–SFO, and HNL–SFO is correlated 0.65 with HNL–SEA. Moreover, correlations are very high between these three routes and other routes that extend well onto the continent: HNL–LAX is correlated 0.81 with HNL–DEN (Denver), 0.82 with HNL–DFW (Dallas–Fort Worth), 0.75 with HNL–ORD (Chicago O’Hare), and 0.73 with HNL–ATL (Atlanta).

That the observed fluctuations in flight times are synchronous throughout the sector regardless of route or carrier suggests a

common driver, which we hypothesize to be climate variability. Correlations of observed atmospheric anomalies with a representative ΔT record (UA HNL–LAX; mean seasonal cycle also removed) reveal the dominant large-scale mechanism. ΔT is anomalously large (that is, eastbound flights are anomalously short and/or westbound flights are anomalously long) when the 300-mb westerly wind between Hawaii and the continental US is anomalously strong (Fig. 2a). Zonal wind correlations of opposite sign immediately poleward and equatorward are a clear manifestation of a cyclonic (anticyclonic) tropospheric circulation anomaly poleward (equatorward) of the airline route (Fig. 2b). This pattern of upper-level zonal wind and mid-tropospheric geopotential height is consistent with the leading modes of Pacific jet stream variability recently identified⁹, and projects strongly onto those associated with ENSO (El Niño phase) and the AO (negative phase) (Supplementary Fig. 1).

To facilitate analysis of the observed temporal covariability of 300-mb zonal wind and ΔT , an index is constructed as the spatially averaged 300-mb zonal wind between Hawaii and the continental US ($u_{300\text{mb}}$; rectangle shown in Fig. 2a). The mean seasonal cycle of $u_{300\text{mb}}$ explains virtually all of the mean seasonality of the flight times (T), flight-time differences (ΔT), and total round-trip flying times (ΣT) (Supplementary Fig. 2). The correlations between $u_{300\text{mb}}$ and ΔT are very high across all timescales down to the highest-frequency fluctuations associated with synoptic weather variability (Fig. 3a). After removing the mean seasonal cycle of both data sets, $u_{300\text{mb}}$ explains 73% of the total daily variance of ΔT and 91% of the interannual variance. Thus, the atmosphere’s well-known influence on aviation transcends from weather to climate timescales.

The 19-year records of observed $u_{300\text{mb}}$ and ΔT also share substantial variance with large-scale modes of tropical and high-latitude climate variability, particularly ENSO and the AO (Fig. 3c). Notably, the largest positive anomalies are coincident with major El Niño events (including 1997–1998 and 2009–2010), and the levelling off at the peak of such anomalies is akin to the AO record. The interannual variability of ΔT is correlated 0.85 with ENSO (0.91 at a 2–3 month lag, due to the observed lag between ENSO and $u_{300\text{mb}}$), and -0.48 with the AO. Indeed, ordinary least-squares multiple linear regression using the NINO3.4 and AO indices as predictors captures 82% of the variance of the observed $u_{300\text{mb}}$ index, and 88% ($r = 0.94$) with NINO3.4 leading by 60 days (Fig. 3d). Interestingly, the difference in westbound and eastbound arrival delays (ΔD , Fig. 3e) is also highly correlated with $u_{300\text{mb}}$ and climate indices, suggesting that natural climate variability (including the seasonal cycle) is not fully accounted for in flight scheduling. Considering that ΔD exceeded 30 min during the 1997–98 and 2009–10 El Niño events, improved seasonal-to-interannual climate predictions (particularly ENSO, for the study region) and their integration into global aviation information systems may yield mutual benefits to society and industry alike.

¹Woods Hole Oceanographic Institution, Woods Hole, Massachusetts 02543, USA. ²Massachusetts Institute of Technology/Woods Hole Oceanographic Institution Joint Program in Oceanography, Cambridge, Massachusetts 02139, USA. ³University of Wisconsin, Madison, Wisconsin 53715, USA.

*e-mail: kk@whoi.edu

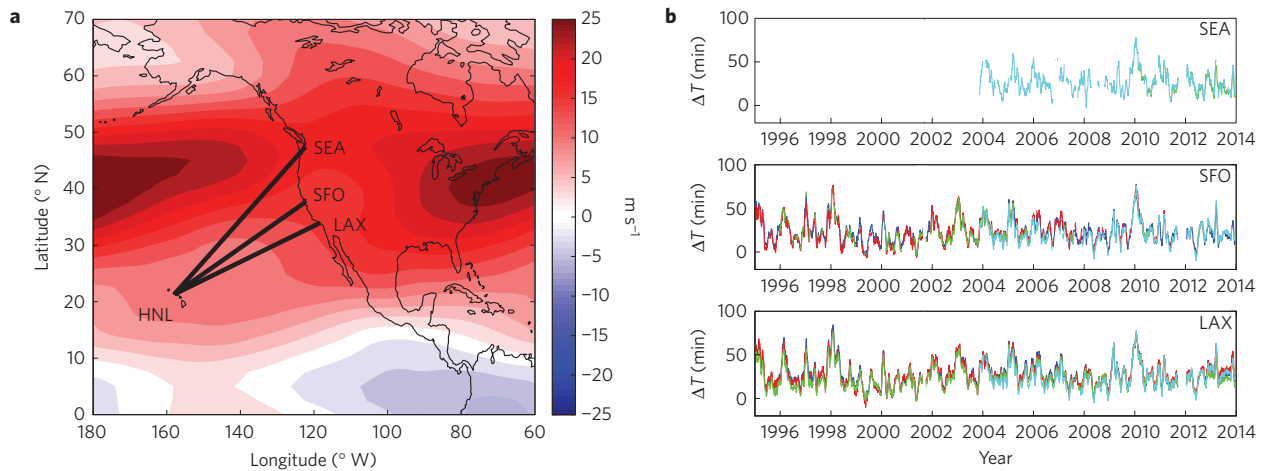


Figure 1 | Overview map and flight-time variability. **a**, Airline routes between HNL and LAX, SFO and SEA International Airports superimposed on the annual mean 300-mb zonal wind field (NCEP/NCAR Reanalysis, 1995–2013). The zonal wind field is contoured every 2.5 m s^{-1} . **b**, Time series of ΔT for the HNL-SEA, HNL-SFO and HNL-LAX routes. Colours in each panel of **b** denote carrier (blue for UA, red for AA, green for DL, and cyan for HA). A 31-day running mean was applied to all time series. No HNL-SEA data were available from UA or AA.

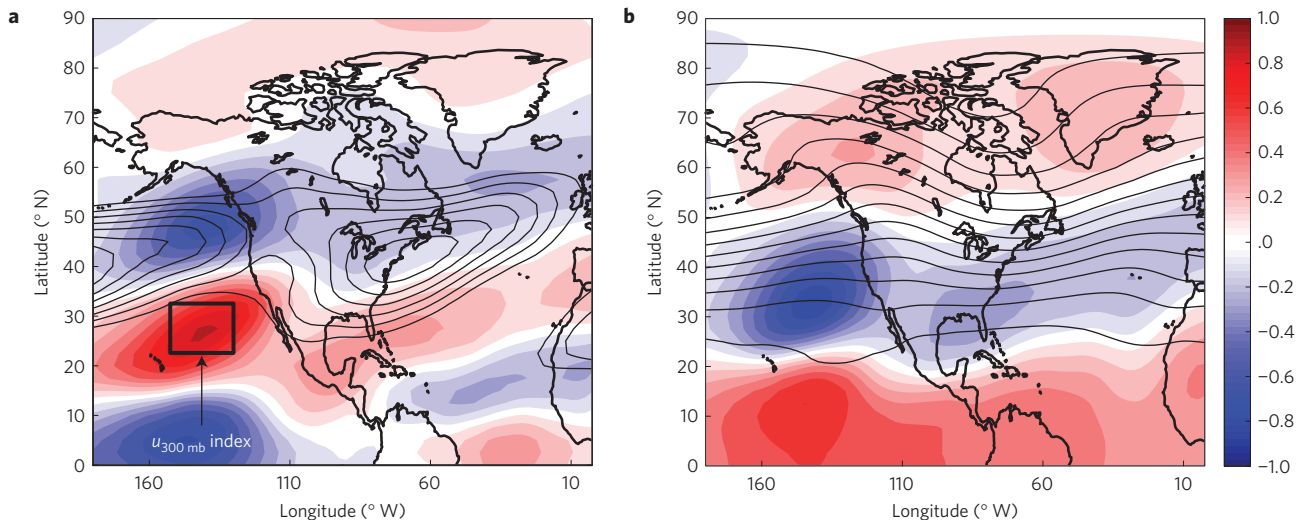


Figure 2 | Atmospheric correlations. **a, b**, Anomaly correlation of the 300-mb zonal wind (**a**) and 500-mb geopotential height fields (**b**) with ΔT for the HNL-LAX route based on UA flights. The mean seasonal cycle was removed from, and a 31-day running mean was applied to, all data. For reference, the annual mean 300-mb zonal wind and 500-mb geopotential height fields are also contoured in black (every 2 m s^{-1} beginning at 5 m s^{-1} and every 50 m beginning at $5,000 \text{ m}$, respectively). The rectangle shown in **a** indicates the region over which 300-mb zonal wind field is spatially averaged to construct the $u_{300\text{mb}}$ index.

Although the Pacific North American pattern also exerts a dominant influence throughout much of the North Pacific sector and may be a valuable predictor of flight statistics for other routes, especially trans-Pacific, its spatial pattern is such that there is negligible impact on 300-mb zonal winds between Hawaii and the continental US, and thus no significant correlation with the routes analysed here. It is also plausible that zonally propagating modes of intraseasonal variability such as the Madden–Julian Oscillation also have a strong impact on air travel in this region, particularly at higher frequencies than those shown in Fig. 3c,d.

Although the relationship between westbound and eastbound flight times is inverse and strong, a closer look at the total round-trip flying time by route (westbound leg plus eastbound leg; ΣT) reveals a small but significant round-trip residual (Fig. 4). The mean residual (that is, the sensitivity of ΣT on the $u_{300\text{mb}}$ index) for the routes and carriers analysed in this study is $0.57 \pm 0.11 \text{ min per m s}^{-1}$. Note that quantitative estimates of this sensitivity must be based

on data before and after mid-2000 separately owing to a systematic jump in flight times across all carriers and routes in both directions (Supplementary Fig. 3). The jump is not related to climate variability, as there is no corresponding jump in $u_{300\text{mb}}$, nor is it a consequence of altered regulations post-9/11, as it occurred roughly one year earlier. Rather, the jump in 2000 is possibly related to a 51% increase in the cost of jet fuel that year, which was the largest annual change since the 1979 energy crisis, and prices continued to rise steadily thereafter (Supplementary Fig. 3, inset). Although the annual cycle contributes a large fraction of shared variance between the full records of ΣT and $u_{300\text{mb}}$ (92% as in Supplementary Fig. 2c,d), statistically significant correlations are maintained after the records are deseasonalized (for example, 0.54 pre-jump), and the regression coefficients are of the same order of magnitude. Reasons for a round-trip residual are elusive to the authors, but it is very robust and implies that changes in flight times and thus fuel consumption, cost and greenhouse gas

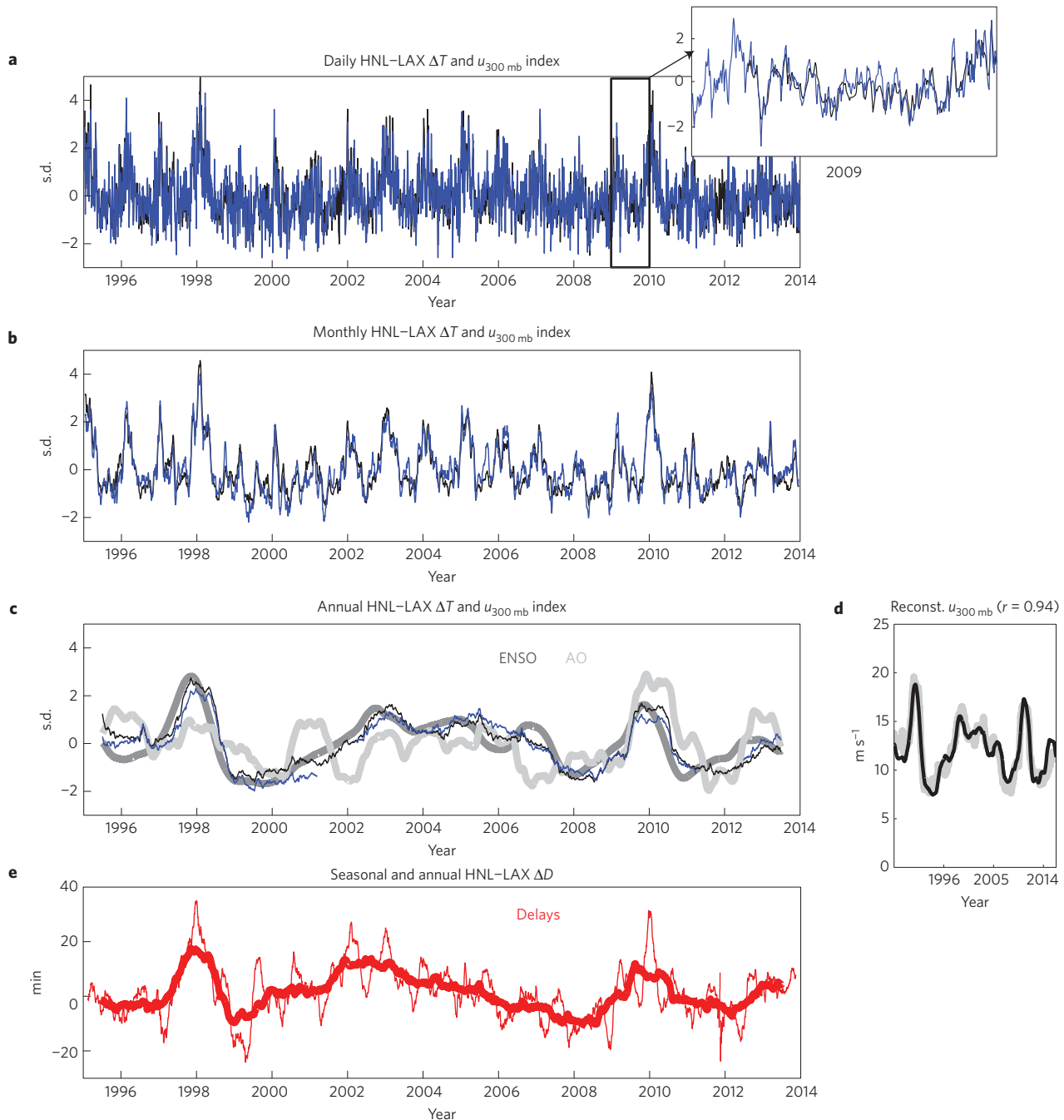


Figure 3 | Flight time, wind and climate. **a–c**, Daily (**a**), monthly (**b**) and annually (**c**) smoothed HNL-LAX (UA) ΔT (blue) and $u_{300\text{mb}}$ index (black). The inset to **a** shows daily ΔT and $u_{300\text{mb}}$ time series for the year 2009. $u_{300\text{mb}}$ versus ΔT correlation coefficients associated with daily, monthly and annually smoothed time series are 0.86, 0.91, and 0.95, respectively. Also shown in **c** are annually smoothed NINO3.4 (dark grey) and AO (light grey; inverted) climate indices. Correlations associated with NINO3.4 are 0.86 and 0.85 for $u_{300\text{mb}}$ and ΔT , respectively (the maximum lead-lag correlation of NINO3.4 and ΔT is 0.91 with NINO3.4 leading by ~ 2.5 months). Correlations associated with the AO are -0.53 and -0.48 for $u_{300\text{mb}}$ and ΔT , respectively. **d**, Observed (grey) and reconstructed (black) annually smoothed $u_{300\text{mb}}$ index based on least-squares multiple linear regression with the NINO3.4 (leading by 60 days) and AO indices as predictors. **e**, Seasonally and annually smoothed HNL-LAX (UA) ΔD for flights that departed on time (± 15 min). ΔD is analogous to ΔT except it refers to the difference in westbound and eastbound arrival delays at the gate relative to scheduled.

emissions do not entirely cancel out as upper-level winds change either as part of natural, oscillatory atmospheric variability or in response to global radiative forcing. It is therefore essential, as a matter of understanding all possible feedbacks between climate and society, to characterize and understand the response of the upper-level wind field to radiative forcing.

Analysing the predicted response of 300-mb zonal winds to increased radiative forcing by 34 global climate models (GCMs)

included in the Coupled Model Intercomparison Project, Phase 5 (CMIP5; ref. 10) paints an uncertain future (Fig. 5a). Under the 8.5 W m^{-2} Intergovernmental Panel on Climate Change (IPCC) forcing experiment (RCP8.5), roughly one-third of GCMs predict a poleward shift (Fig. 5c), one-fifth predict an equatorward shift (Fig. 5d), and the remaining half predict only a very small or insignificant change in the latitudinal position or strength of the annual mean Pacific jet. However, the most robust aspect of

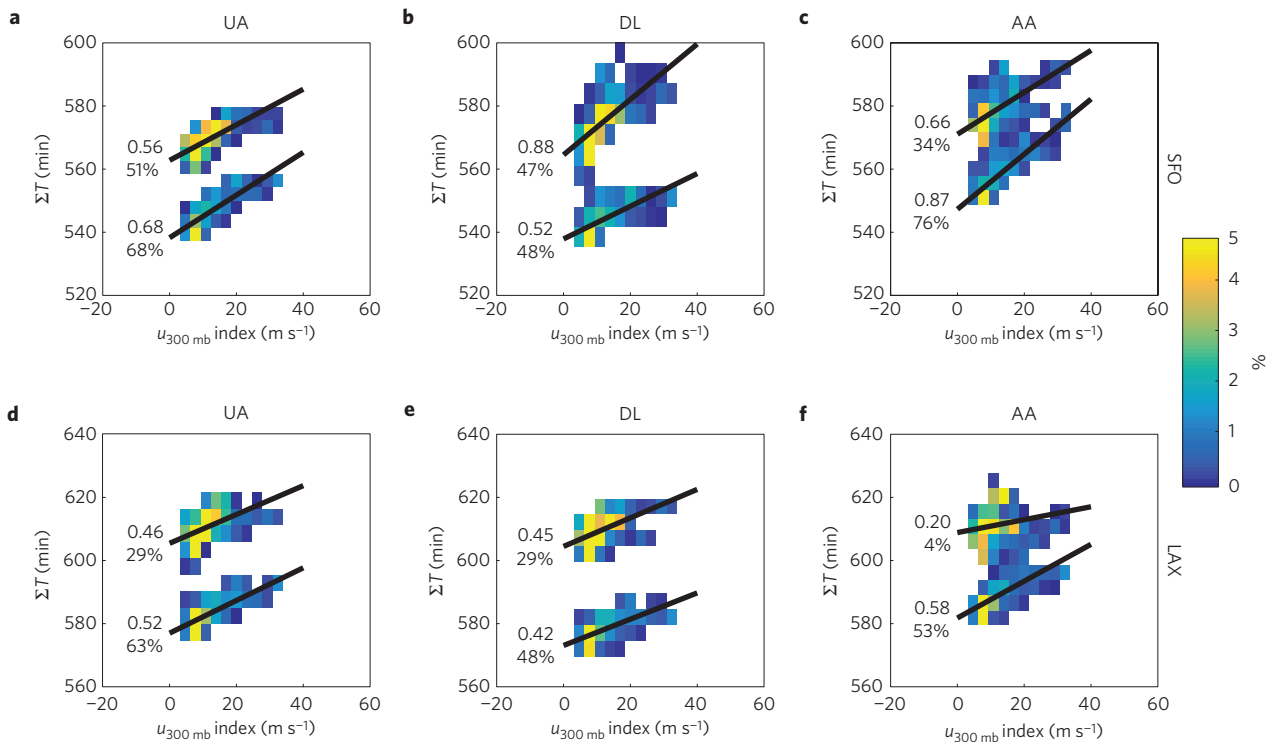


Figure 4 | Round-trip flying time residual. **a–f**, Scatter density plots of the seasonal (91-day running mean) ΣT as a function of the $u_{300\text{mb}}$ index (rectangle shown in Fig. 2a). Routes are by rows (top row, **a–c**, for HNL-SFO; bottom row, **d–f**, for HNL-LAX), and columns are by carrier (UA, DL and AA, from left to right). The residual rate dependence of ΣT on $u_{300\text{mb}}$ is given by the slope of each black line (minutes ΣT per $\text{m s}^{-1} u_{300\text{mb}}$), estimated by ordinary least-squares linear regression, and is indicated next to each line along with the percentage of variance explained ($100 * r^2$). Bold numbers indicate correlations that are significant at the 95% confidence level, accounting for the effective degrees of freedom. The bottom (top) groups of data in each panel are data before (after) the system-wide shift in mean ΣT that occurred in mid-2000; see Supplementary Fig. 3.

the projected change in the annual mean 300-mb zonal wind field over the North Pacific sector—consistent across half of the GCMs—is a zonal extension of the jet exit region into the corridor between Hawaii and the continental US ($1.6 \pm 0.4 \text{ m s}^{-1}$ local increase in annual mean 300-mb zonal wind ($u_{300\text{mb}}$ index); Fig. 5e). The multi-model ensemble projections shown in Fig. 5 based on CMIP5 models are consistent with previous assessments of CMIP3 and CMIP5 models^{11–13} and, together with these studies, underscore the importance of GCMs to reliably predict the future state of the tropical Pacific Ocean. On the basis of the observed empirical relationships discussed above and shown in Fig. 4, such a change in annual mean upper-level winds would result in ~ 5.5 additional flying hours per daily round-trip, per carrier, per comparable route, per year. Assuming twice-daily round-trip flights, and just the four carriers and three routes analysed here yields 133 additional flying hours per year, which amounts to roughly 480,000 US gallons (gal) jet fuel consumed (at 1 gal per s), $\sim \text{US}\$1.4$ million fuel cost (at $\text{US}\$3$ per gal), and 4.6 million kg CO_2 emitted per year (at 9.6 kg CO_2 per gal). Multi-model projections focusing on the boreal winter season, which is the season of maximum climatological jet strength, are much larger and more robust across models (Fig. 5b). The multi-model median change in 300-mb zonal wind between Hawaii and the continental US ($u_{300\text{mb}}$ index) during boreal winter is $5.0 \pm 1.4 \text{ m s}^{-1}$ (104 additional flying hours, 373,000 gal jet fuel consumed, $\text{US}\$1.1$ million fuel cost, and 3.6 million kg CO_2 emitted per winter under the same assumptions).

Although an additional 4.6 million kg CO_2 is extremely small compared with the total global emissions by all anthropogenic sources, that calculation is based on only three US domestic routes where zonal wind anomalies have a significant influence. Extrapolation to the global commercial airline industry is not

straightforward, because neither wind changes nor airline routes are uniformly distributed, but an order-of-magnitude perspective can be offered. In 2014, there are an estimated 49,871 routes served by commercial airlines, with 102,470 flights per day ($\sim 30,000$ commercial flights per day in the US domestic market). For an average change in total round-trip flying time by route (ΣT) of one minute, commercial jets would be in the air $\sim 300,000$ h longer per year, amounting to ~ 1 billion additional gal jet fuel ($\sim \text{US}\$3$ billion fuel cost), and 10,000 million kg CO_2 emitted, per year. Such an additional annual CO_2 emission is equivalent to 1.5% of CO_2 emissions by the global commercial airline industry, and 0.03% of global CO_2 emissions by all anthropogenic sources. The potential feedback arises as the added emissions amplify the incipient changes in atmospheric circulation, and so forth.

Given the observed dependence of flight times on 300-mb zonal winds (Fig. 3), the level of variability of upper-level winds is also germane to airline operations—analogueous to volatility in a market or in the price of raw materials. It is well known that synoptic-scale weather variability is significantly more energetic during wintertime (Supplementary Fig. 4a); so, too, is the daily-scale variability in flight times (Supplementary Fig. 4b). At the interannual timescale, the daily-scale variance in $u_{300\text{mb}}$ also proves to be modulated by the phase of the AO; the variance of $u_{300\text{mb}}$ is anomalously large when the AO is in a negative phase (Supplementary Fig. 4c,d). Also, although the monthly variability of $u_{300\text{mb}}$ is projected to become stronger in general (Supplementary Fig. 4e), the deseasonalized anomalies do not show such a change (Supplementary Fig. 4f), implying a stronger annual cycle. The lack of a robust projected change in the amplitude of interannual variability of $u_{300\text{mb}}$ (Supplementary Fig. 4f) is qualitatively consistent with IPCC syntheses noting the lack of robust changes in the amplitude of ENSO and the AO.

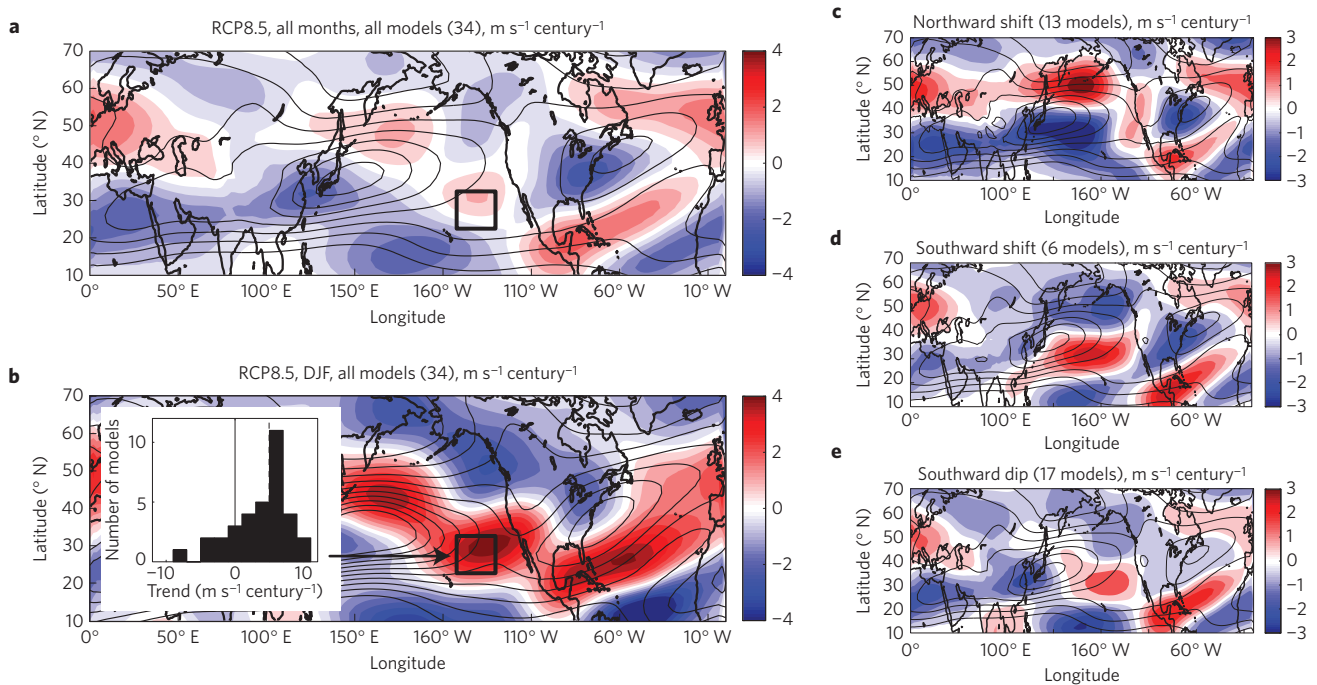


Figure 5 | Projected trends in mean flight-level winds. **a**, CMIP5 multi-model ($N=34$) mean trend in 300-mb zonal wind under the IPCC AR5 RCP8.5 future forcing experiment (2006–2100). For reference, the multi-model, annual mean 300-mb zonal wind field is also contoured in black (every 5 m s^{-1} beginning at 5 m s^{-1}). **b**, The same as in **a** but for the boreal winter season (December–February). **c**, The same as in **a** but including only those models that predict a northward shift of the annual mean Pacific jet stream ($N=13$). **d**, The same as in **a** but including only those models that predict a southward shift of the annual mean Pacific jet stream ($N=6$). **e**, The same as in **a** but including only those models that predict a pronounced southward dip of the annual mean Pacific jet stream ($N=17$). The inset in **b** shows a histogram of projected trends in boreal winter $u_{300\text{mb}}$. The solid and dashed vertical lines represent zero and the median projected $u_{300\text{mb}}$ trend, respectively.

It is clear that the acute sensitivity of the commercial airline industry to atmospheric variability extends beyond ‘weather’—to the seasonal and interannual (‘climate’) timescales. Synoptic weather patterns, the annual cycle of solar forcing, and modes of interannual climate variability such as ENSO and the AO control the strength and variance of flight-level winds, and flight-level winds seem to be the overwhelmingly dominant predictor of flight durations. Climate mechanisms that dictate the variability of flight times in other busy regions such as the North Atlantic, Europe and Asia are likely to differ in details from those identified herein but still probably boil down to what controls flight-level winds between airports. Although much of the discussion of the relationship between climate change and air travel focuses on the contribution of global aviation to radiative forcing (greenhouse gases and contrails), the findings presented here suggest that more complex feedbacks may be at play. In particular, radiatively forced changes in circulation have the potential to influence the rate of consumption of fossil fuels by the airline industry (initially by up to a few per cent), thus feeding back onto the global radiative forcing and resultant changes in circulation. Central to this feedback is the residual dependence of total flying time on flight-level winds, the dynamics of which warrant further investigation.

Received 14 July 2014; accepted 9 June 2015;
published online 13 July 2015

References

- Horel, J. D. & Wallace, J. M. Planetary-scale atmospheric phenomena associated with the southern oscillation. *Mon. Weath. Rev.* **109**, 813–829 (1981).
- Seager, R., Harnik, N., Kushnir, Y., Robinson, W. & Miller, J. Mechanisms of hemispherically symmetric climate variability. *J. Clim.* **16**, 2960–2978 (2003).
- Thompson, D. W. J. & Wallace, J. M. Annular modes in the extratropical circulation. Part I: Month-to-month variability. *J. Clim.* **13**, 1000–1016 (2000).

- Solomon, S. *et al.* (eds) *Climate Change 2007: The Physical Science Basis* (IPCC, Cambridge Univ. Press, 2007).
- Burkhardt, U. & Karcher, B. Global radiative forcing from contrail cirrus. *Nature Clim. Change* **1**, 54–58 (2011).
- Williams, P. D. & Joshi, M. M. Intensification of winter transatlantic aviation turbulence in response to climate change. *Nature Clim. Change* **3**, 644–648 (2013).
- Wolff, J. K. & Sharman, R. D. Climatology of upper-level turbulence over the contiguous United States. *J. Appl. Meteorol. Clim.* **47**, 2198–2214 (2008).
- Kalnay, E. *et al.* The NCEP/NCAR 40-year reanalysis project. *Bull. Am. Meteorol. Soc.* **77**, 437–471 (1996).
- Jaffe, S. C., Martin, J. E., Vimont, D. J. & Lorenz, D. J. A synoptic climatology of episodic, subseasonal retractions of the Pacific jet. *J. Clim.* **24**, 2846–2860 (2011).
- Taylor, K. E., Stouffer, R. J. & Meehl, G. A. An overview of Cmp5 and the experiment design. *Bull. Am. Meteorol. Soc.* **93**, 485–498 (2012).
- Delcambre, S. C., Lorenz, D. J., Vimont, D. J. & Martin, J. E. Diagnosing northern hemisphere jet portrayal in 17 CMIP3 global climate models: Twenty-first-century projections. *J. Clim.* **26**, 4930–4946 (2013).
- Delcambre, S. C., Lorenz, D. J., Vimont, D. J. & Martin, J. E. Diagnosing northern hemisphere jet portrayal in 17 CMIP3 global climate models: Twentieth-century intermodel variability. *J. Clim.* **26**, 4910–4929 (2013).
- Barnes, E. A. & Polvani, L. Response of the midlatitude jets, and of their variability, to increased greenhouse gases in the CMIP5 models. *J. Clim.* **26**, 7117–7135 (2013).

Acknowledgements

The authors thank B. Carmichael and B. Sharman of the National Center for Atmospheric Research Aviation Applications Program, G. Compo of the Cooperative Institute for Research in the Environmental Sciences, and D. Battisti of the University of Washington Department of Atmospheric Sciences for helpful discussions. We acknowledge the World Climate Research Programme’s Working Group on Coupled Modelling, which is responsible for CMIP5, and we thank the climate modelling groups for producing and making available their model output. For CMIP5, the US Department of Energy’s Program for Climate Model Diagnosis and Intercomparison provides coordinating support and led development of software infrastructure in partnership with the Global Organization for Earth System Science Portals. CMIP5 model output data were acquired from the WHOI CMIP5 Community Storage Server, Woods Hole Oceanographic Institution, Woods Hole, Massachusetts, USA. NCEP/NCAR Reanalysis

data were provided by the NOAA/OAR/ESRL PSD, Boulder, Colorado, USA, and acquired from their website at <http://www.esrl.noaa.gov/psd>. Domestic flight data were acquired from the TranStats website, maintained by the Bureau of Transportation Statistics, Research and Innovative Technology Administration (RITA), US Department of Transportation (<http://www.transtats.bts.gov>). Airline industry and business statistics were gathered from the MIT Global Airline Industry Program, Airline Data Project (<http://web.mit.edu/airlinedata/www/Revenue&Related.html>), Air Transport Action Group (http://aviationbenefits.org/media/26786/ATAG__AviationBenefits2014_FULL_LowRes.pdf), and National Air Traffic Controllers Association (NATCA). Emissions coefficients were gathered from the US Energy Information Administration (http://eia.gov/environment/emissions/co2_vol_mass.cfm). K.B.K. acknowledges support from the Strategic Environmental Research and Development Program, the WHOI Oceans and Climate Change Institute, the Alfred P. Sloan Foundation, and Microsoft Research.

Author contributions

K.B.K. and H.C.B. jointly conceived the study. K.B.K. conducted the analyses and wrote the paper with input from all authors.

Additional information

Supplementary information is available in the online version of the paper. Reprints and permissions information is available online at www.nature.com/reprints. Correspondence and requests for materials should be addressed to K.B.K.

Competing financial interests

The authors declare no competing financial interests.